Science of the Total Environment 651 (2019) 1166–1179

Contents lists available at ScienceDirect

Science of the Total Environment

journal homepage: www.elsevier.com/locate/scitotenv

Testing the performance of sensors for ozone pollution monitoring in a citizen science approach

A. Ripoll [a], M. Viana [a,*], M. Padrosa [a], X. Querol [a], A. Minutolo [b], K.M. Hou [c], J.M. Barcelo-Ordinas [d], J. Garcia-Vidal [d]

[a] Institute of Environmental Assessment and Water Research (IDAEA-CSIC), 08034 Barcelona, Spain
[b] Legambiente Onlus, 00199 Rome, Italy
[c] LIMOS Laboratory, UMR 6158, CNRS, Centre National de la Recherche Scientifique, Clermont-Ferrand, France
[d] Department of Computer Architecture, Universitat Politècnica de Catalunya (UPC), 08034 Barcelona, Spain

HIGHLIGHTS

- Citizen science is useful for awareness raising, if sensors are validated.
- Performance of 143 ozone electrochemical and metal-oxide sensors was tested.
- R^2 between sensor and reference data was 0.88 (0.78–0.96) and 0.89 (0.73–0.96).
- Sensors tested are useful to communicate daily means but not peak episodes.
- Uncertainties must always be communicated to the public.

GRAPHICAL ABSTRACT

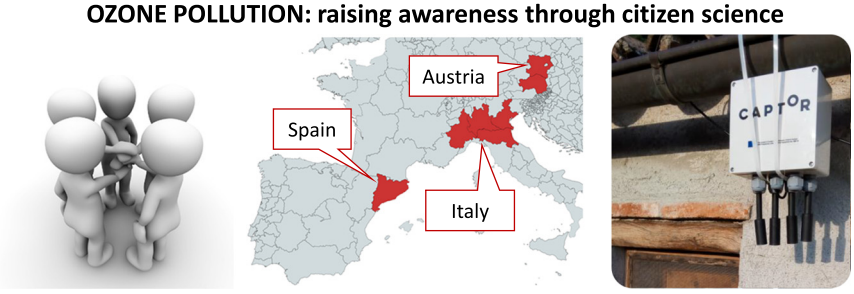

ARTICLE INFO

Article history:
Received 9 July 2018
Received in revised form 13 September 2018
Accepted 20 September 2018
Available online 22 September 2018

Editor: Lidia Morawska

Keywords:
Uncertainty
Low-cost sensors
Validation
Performance
Awareness
Platform
Node

ABSTRACT

Tropospheric ozone (O_3) is an environmental pollutant of growing concern, especially in suburban and rural areas where the density of air quality monitoring stations is not high. In this type of areas citizen science strategies can be useful tools for awareness raising, but sensor technologies must be validated before sensor data are communicated to the public. In this work, the performance under field conditions of two custom-made types of ozone sensing devices, based on metal-oxide and electrochemical sensors, was tested. A large array of 132 metal-oxide (Sensortech MICS 2614) and 11 electrochemical (Alphasense) ozone sensors, built into 44 sensing devices, was co-located at reference stations in Italy (4 stations) and Spain (5). Mean R^2 between sensor and reference data was 0.88 (0.78–0.96) and 0.89 (0.73–0.96) for Captor (metal-oxide) and Raptor (electrochemical) nodes. The metal-oxide sensors showed an upper limit (approximately 170 μg/m^3) implying that these sensors may be useful to communicate mean ozone concentrations but not peak episodes. The uncertainty of the nodes was 10% between 100 and 150 μg/m^3 and 20% between 150 and 200 μg/m^3, for Captors, and 10% for >100 μg/m^3 for Raptors. Operating both types of nodes up to 5 months did not evidence any clear influence of drifts. The use of these sensors in citizen science can be a useful tool for awareness raising. However, significant data processing efforts are required to ensure high data quality, and thus machine learning strategies are advisable. Relative uncertainties should always be reported when communicating ozone concentration data from sensing nodes.

* Corresponding author.
E-mail address: mar.viana@idaea.csic.es (M. Viana).

https://doi.org/10.1016/j.scitotenv.2018.09.257

1. Introduction

Tropospheric ozone (O_3) is a secondary pollutant formed through chemical reactions of gaseous precursors in the presence of sunlight. Its complex formation mechanisms are based on the photo-oxidation of volatile organic compounds (VOCs) and nitrogen oxides (NO_x) (Millán et al., 2000; Monks et al., 2015; Pusede et al., 2015; Richards et al., 2013; Sillman, 1999), and both types of precursors may have natural (biogenic) and anthropogenic origin (Varinou et al., 1999). Part of the complexity of this atmospheric pollutant is linked to the lack of linearity of its formation pathways (Monks et al., 2015; Pusede et al., 2015; Sillman, 1999), as NO_x are also involved in ozone removal through titration with nitrogen monoxide (NO) to form nitrogen dioxide (NO_2) (Mészáros, 1999). Ozone formation processes are intensified with high insolation in summer, resulting in characteristic ozone episodes especially in Southern Europe (Cristofanelli and Bonasoni, 2009; Gangoiti et al., 2001; Gerasopoulos et al., 2006; Millán et al., 1991; Querol et al., 2016; among others). Because of its chemical properties, ozone is hazardous in the lower troposphere to human health (HEI, 2017; WHO, 2008) and ecosystems (Nali et al., 2002).

Ozone dynamics are strongly dominated by air mass transport from regions where precursors are emitted (typically, urban areas) to regions where ozone exposures occur (typically, suburban and rural areas). Examples of this kind of pattern, where the populations affected by ozone episodes are not generally responsible for the emission of its precursors, are frequently found in the literature especially in coastal areas where emissions are transported inland by the sea breeze (Millán et al., 2000; Querol et al., 2017). Although this kind of regional ozone production may decisively contribute (Querol et al., 2016) to the exceedances of the ozone information threshold (180 μg/m^3, as established by EU Directive 92/72/EEC), population awareness regarding ozone pollution is generally low in rural areas. The lower population density in these areas is reflected in a lower number of reference air quality monitoring stations, and this may result in lower political and environmental pressure for action.

In this type of lower density population areas, citizen science strategies can be useful tools for awareness raising. Citizen science approaches, and more specifically sensor technologies, are currently the focus of an increasing number of studies targeting diverse environmental pollutants (WMO, 2018). The concept of "fit for purpose" is frequently addressed, referring to the fact that the quality of the data generated by the sensors should be in accordance with their purpose (e.g., air quality assessment, public information, awareness raising, etc.) (Morawska et al., 2018). Different sensing technologies are available commercially and at development stage from universities and technology centres, with varying results with regard to the quality of the data generated by the sensors (Moltchanov et al., 2015; Jiao et al., 2016; Lin et al., 2017; Nakayama et al., 2017; Zikova et al., 2017; WMO, 2018; Lin et al., 2017, 2015; Spinelle et al., 2015a, b, 2017; Williams et al., 2013, 2014; Borghi et al., 2017; Morawska et al., 2018; Kizel et al., 2018 among others). Testing of low-cost ozone sensors under controlled laboratory conditions has shown good correlations ($R^2 > 0.90$) with reference measurements (Rai et al., 2017). However, their performance decreases significantly under field conditions ($R^2 =$ 0.01–0.94) (Broday et al., 2017; Mukherjee et al., 2017; among others). This decrease is mainly related to interference with other pollutants and with meteorological conditions (Aleixandre and Gerboles, 2012; Spinelle et al., 2015a, b, 2017; WMO, 2018). Different interpretations are also being put forward regarding their applications (Haklay, 2015; Hubbell et al., 2018; Morawska et al., 2018; WMO, 2018), e.g., regarding the method and degree that citizen science is integrated into local, city, national, and international policy level (Haklay, 2015) or how the introduction of sensors may change the relationship between communities and air quality managers (Hubbell et al., 2018). Over all, there is a general call for precaution from the atmospheric research community to validate the performance of such low-cost sensors (Lewis and Edwards, 2016; WMO, 2018). Because of the potentially large datasets produced and the influence of numerous pollutant interferences, machine learning approaches such as artificial neural networks, boosted regression trees and Gaussian processes emulation are being proposed for data evaluation (Lewis et al., 2016; Smith et al., 2017; Spinelle et al., 2017; WMO, 2018; Zimmerman et al., 2018).

In this framework, this work aims to test the performance under field conditions of two custom-made types of ozone sensing devices, based on metal-oxide and electrochemical sensors. The sensors were built for H2020 project CAPTOR (www.captor-project.eu) and deployed in three European countries (Spain, Austria, Italy) with a citizen science approach, aiming to raise awareness about ozone pollution. The ultimate goal of the project was to provide ozone concentration data to citizens in the study regions. To this end, the sensor nodes were intercompared with ozone reference instrumentation under characteristic summer atmospheric conditions in two of the three study areas (Spain and Italy), with the results presented in this work.

2. Methodology

2.1. Study areas

Inter-comparisons between sensor nodes and reference instruments were carried out in Spain and Italy, with the aim to challenge the nodes with diverse environmental conditions. The Spanish study area, covering an approximate area of 90 km × 20 km in central Catalonia (NE Spain, Fig. 1), typically records the highest ozone concentrations in Spain according to reference air quality monitoring stations (EEA, 2017; Querol et al., 2016). This is mainly due to the influence of the Barcelona city pollution plume and to the peculiar local orography and meteorology (ETC, 2018; Querol et al., 2017). The hourly information threshold for ozone (180 μg/m^3) was exceeded 53 times in this area during 2017, and the maximum hourly concentration recorded was 223 μg/m^3 (Table 1). The Italian study area is located in the north of the country and it is comprised of 4 sub-regions (Piedmont, Lombardy, Emilia Romagna and Veneto) of approximately 22,000 km^2 each. It includes the Po Valley, one of the most polluted areas in Europe (European Environment Agency, 2017) where the hourly information threshold was exceeded 85 times in 2017 and ozone concentrations reached up to 248 μg/m^3 (Table 1).

2.2. Ozone sensor nodes

Two different types of low-cost sensor nodes were tested for ambient air ozone monitoring. Irrespective of the sensor technology used (metal-oxide or electrochemical, see below), each node comprised several sensing units, an external power source and an enclosure with data transmission capabilities. The nodes using metal-oxide sensors are referred to as Captors, while those using electrochemical sensors are referred to as Raptors.

2.2.1. Captor nodes

33 Captor nodes were tested. Captor nodes were developed by the Universitat Politecnica de Catalunya (UPC) and consist of a box with 4 SGX Sensortech MICS 2614 metal-oxide ozone sensors, 1 air temperature (T) and 1 air relative humidity (RH) sensor (DHT1 Grove). The sensors were soldered on to an electronic board circuit which is connected to an Arduino Yun platform. 3G USB connection with a global telecom operator is the main communication channel, although they can also use Wifi connection. The electronic board and communication chipsets are fixed inside the box (Fig. S1). Resistance values (kOhm) reflecting ozone concentrations were recorded with a 1-minute time resolution, and averaged over 30-minute periods. The raw data (kOhm) were stored in a csv file and transmitted to a central server.

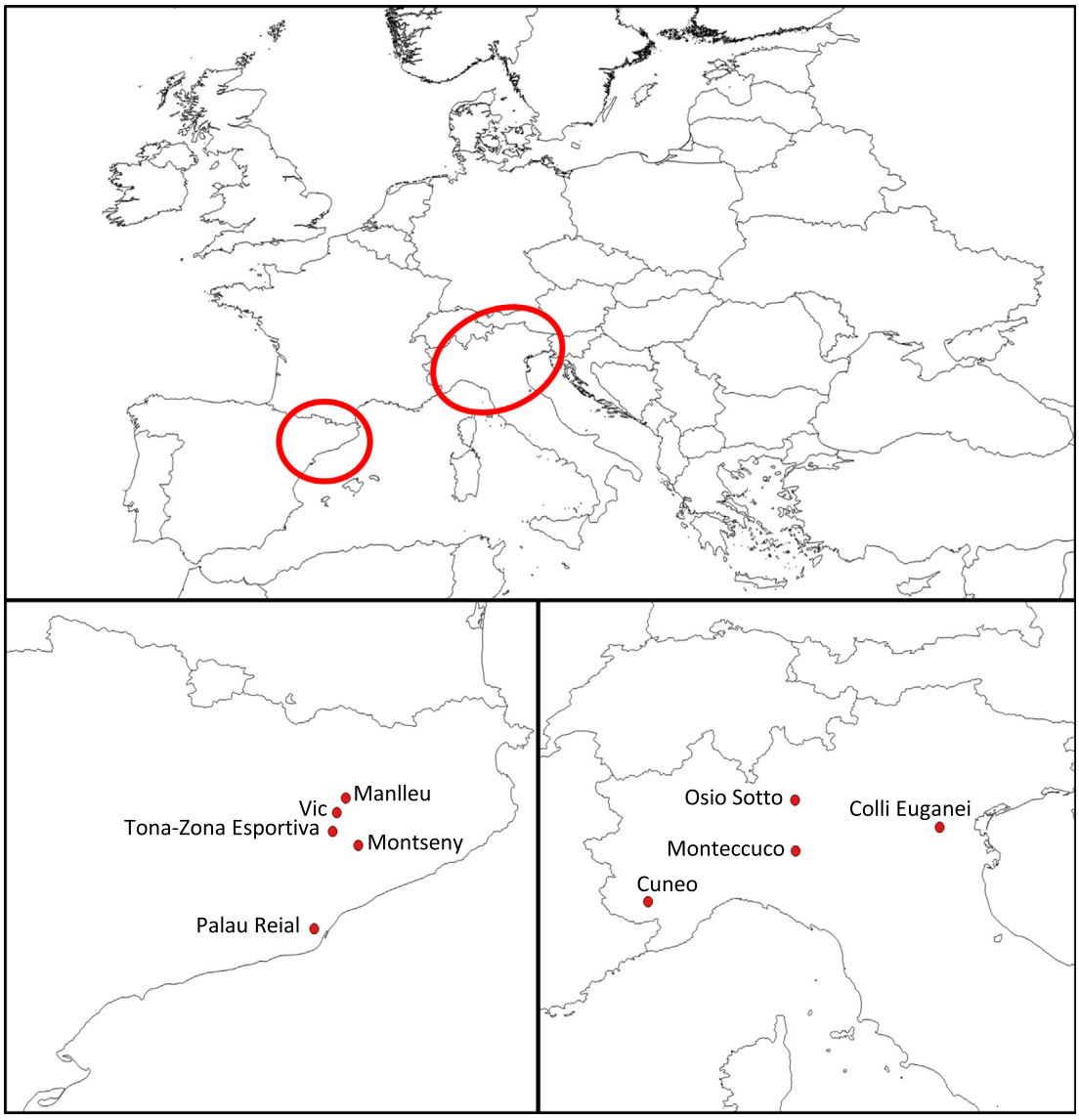

Fig. 1. Top: location of the two study areas. Bottom: location of the 5 reference stations in Spain (left) and the 4 in Italy (right).

Table 1
Air quality monitoring reference stations used in this work.

Code	Name	Location	Coordinates UTM (m)	Elevation (masl)	Study areas	Pollutant situation	Hours with O_3 higher than 180 μg/m^3 in 2017	Hourly max concentration in 2017
MAN	Manlleu (hospital comarcal)	Manlleu	440960, 4650395	460	Spain	Suburban background	7	201
VIC	Vic (estadi)	Vic	436986, 4642840	498	Spain	Suburban background	12	206
TON	Tona (zona esportiva)	Tona	435035, 4633053	620	Spain	Rural background	27	223
MSY	La Castanya	Montseny	446649, 4625477	693	Spain	Rural background	7	193
PR	Palau Reial	Barcelona	426062, 4582127	81	Spain	Urban background	–	–
PM	Parco Monteccuco	Piacenza	500000, 4982950	61	Italy	Urban background	21	202
CUN	Alpini	Cuneo	383575, 4915293	553	Italy	Urban background	–	–
OS	Osio Sotto	Osio Sotto	547691, 5052072	182	Italy	Suburban background	43	248
CE	Colli Euganei	Cinto Euganei	707237, 5018513	12	Italy	Rural background	21	207

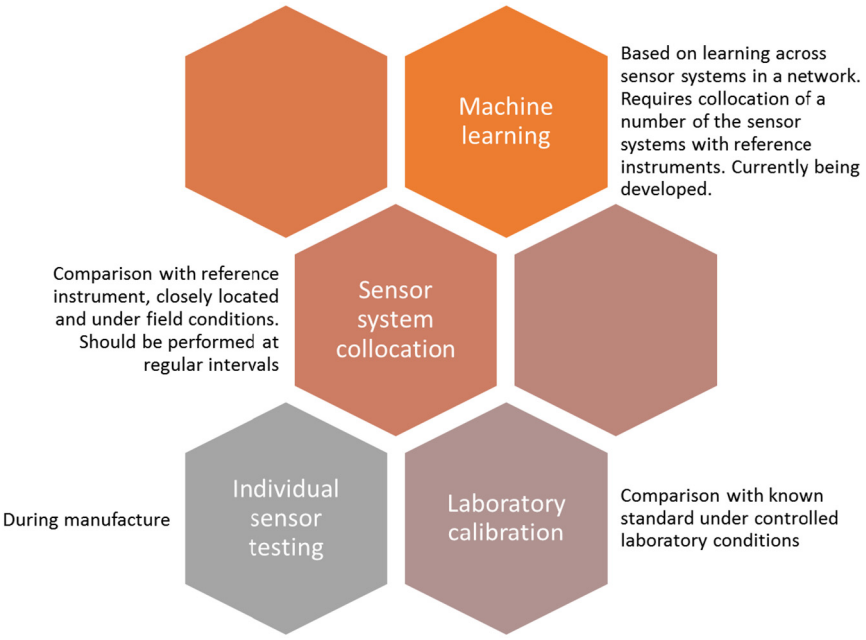

Fig. 2. Alternative methods available for calibration of low-cost sensor systems.

2.2.2. Raptor nodes

11 Raptor nodes were tested. Raptor nodes (hardware and software) were developed by the SMIR group of the laboratory of LIMOS of University Clermont Auvergne (UCA). A Raptor platform consists of a Raptor Local Server (RLC) and at least one Raptor End-Device (RED), maximum number of RED for RLC is 20. The RLC is built by using one uSu-Edu board and one Raspberry Pi 3 board, equipped with a 3G/4G modem for internet connection. Notice that Ethernet and Wi-Fi may also be used for internet connection. The RED is based on uSu-Edu board designed by UCA and equipped with 1 Alphasense's electrochemical ozone sensor (OX-B431), 1 Alphasense's electrochemical nitrogen dioxide sensor (NO2-B43F), 1 air temperature and 1 air relative humidity sensor (Fig. S1). The default sample period of sensory data is 1 min and it may be reconfigured. The raw sensory data is sent to RLC through IEEE802.15.4. The RLC processes the raw sensory data before sending to the remote servers: UCA remote server. An API was developed to enable users to access in near real-time to the raw and calibrate data from the UCA remote server.

2.3. Field testing

Data quality is assessed as a function of sensor sensitivity, selectivity, temporal resolution, reproducibility, and stability over time (WMO, 2018). These assessments are carried out by comparing sensor data with those from reference instrumentation, under conditions which may range from laboratory to environmental, and using different degrees of signal processing. Each of these options has different requirements and results in varying degrees of data quality (Fig. 2). In this work, the performance of 33 Captor and 11 Raptor nodes (132 metal-oxide ozone sensors and 11 electrochemical ozone sensors) was tested between May and October 2017 by comparison with ozone reference data from 5 local air quality monitoring stations in Spain and 4 in Italy (Fig. 1, Tables 1 and S1 in Supporting information). All of the air quality monitoring stations are equipped with reference instrumentation for ozone monitoring according to Directive 2008/50/EC.

- In Spain: Manlleu suburban background station (7 Captor nodes), Vic suburban background station (1 Captor), Tona rural background station (10 Captors and 1 Raptor), Montseny rural background station (1 Captor), and Palau Reial urban background station (6 Captors and 1 Raptor) (Table S1).

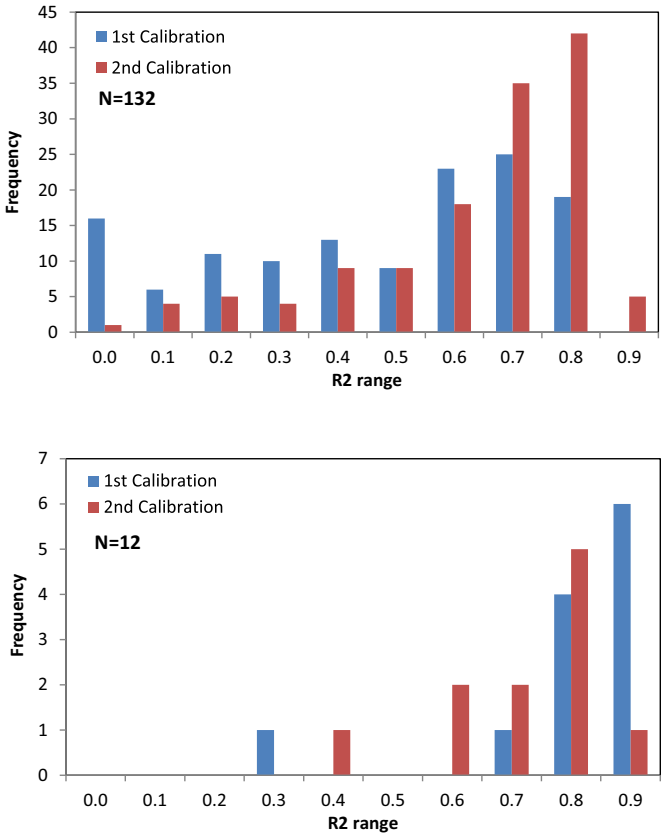

Fig. 3. Frequency distribution of the correlation coefficients of each individual metal-oxide (top) and electrochemical (bottom) sensor during first and second calibration.

- In Italy: Montecucco urban background station (3 Captor and 2 Raptor nodes), Cuneo urban background station (3 Captors and 2 Raptors), Osio Sotto suburban background station (1 Captors and 3 Raptors), and Colli Euganei rural background station (1 Captor and 3 Raptors) (Table S1).

The nodes were deployed following two different strategies (Table S1 in Supporting information): 8 of the 33 Captors and 4 of the 11 Raptors were collocated at the reference stations during the entire monitoring period (May to October 2017, 6 months). In addition, 25 Captors and 7 Raptors were collocated during intensive 2-week

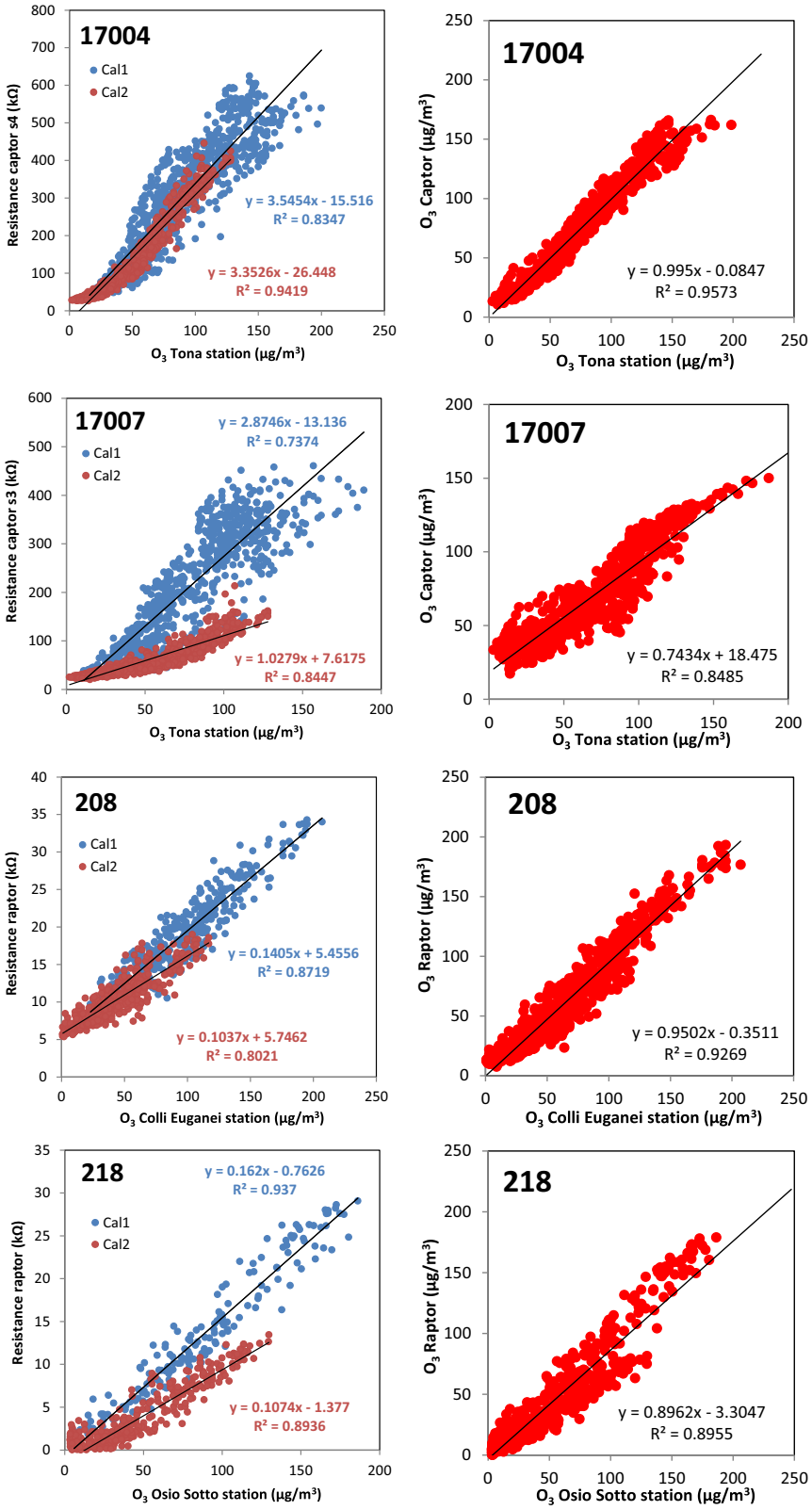

Fig. 4. Scatter plots of the ozone sensors raw data (left) and ozone sensors calculated mass concentration (right) vs. ozone reference concentrations.

campaigns (referred to as first and second calibration) before and after the summer period (between May and July, and in September and October).

2.4. Data processing

After the collocation period, a dataset was obtained for each node including date stamp, ozone concentration from the reference station, raw data (resistance values, kOhm) from the four ozone metal-oxide sensors (referred to as s1, s2, s3, s4), T and RH, for the Captor nodes. A similar dataset was obtained for the Raptor nodes, although with only one electrochemical ozone sensor raw data and in addition with nitrogen dioxide from the reference station and raw data from the nitrogen dioxide electrochemical sensor. Each individual sensor inside each node (in total, 132 metal-oxide and 11 electrochemical ozone sensors) was calibrated for each of the calibration periods.

Each dataset was divided into two, defined as the training and the validation (or testing) sets. Prior to this division the data were shuffled

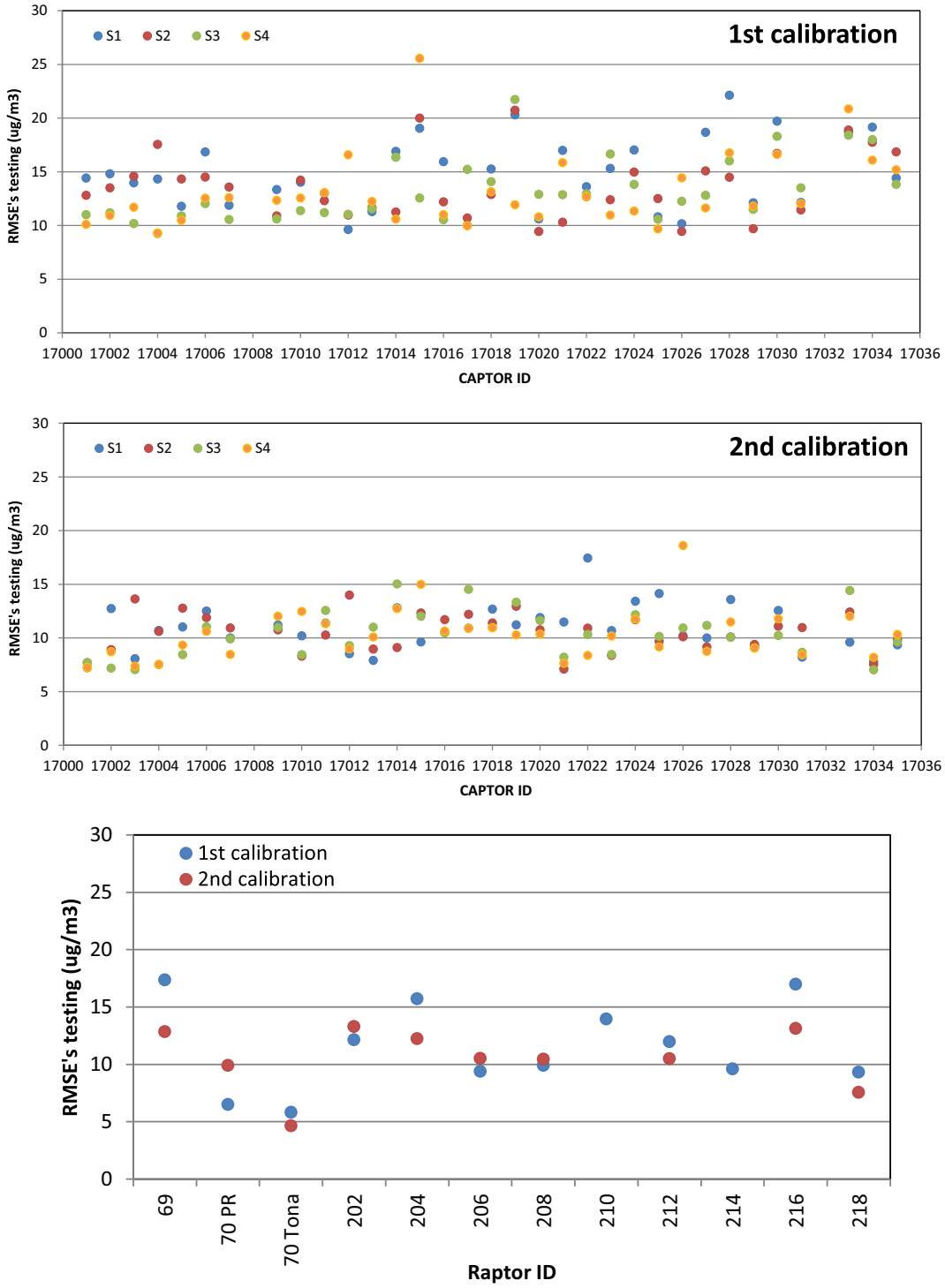

Fig. 5. Root Mean Square Error (RMSE) calculated for the testing dataset during the first and second calibrations for metal-oxide (top and middle) and electrochemical (bottom) sensors.

in order to randomly include high and low ozone concentrations in both subsets of data. The sensors were then calibrated with the results from the training set, and the goodness of the fit with regard to reference data was quantified by applying the calibration coefficients obtained with the training set to the validation set (Hastie et al., 2001).

Calibration was carried out applying Multiple Linear Regression (MLR) to the training datasets of each individual ozone sensor, by regressing the raw data (in units of electrical resistance) against the simultaneous reference ozone concentrations (μg/m^3). Temperature and RH were included in the model as dependent variables, and also nitrogen dioxide in the case of Raptors. In order to do this, all datasets were previously normalized with respect their mean and standard deviation. MLR then produced normalized coefficients (referred to as "beta" coefficients) for each individual ozone, T and RH sensor in the Captor nodes (and ozone, nitrogen dioxide, T and RH for the Raptor nodes). In total, four ozone regression coefficients were calculated for the Captor nodes, and 1 for Raptor nodes, for each of the calibration periods (first and second calibration).

Subsequently, ozone concentrations for each individual sensor were calculated by denormalizing the data using the following equations:

$$X_{O3Rnorm} = (X_{O3R} - \mu_{O3R})/\sigma_{O3R} \quad (1)$$

$$X_{NO2Rnorm} = (X_{NO2R} - \mu_{NO2R})/\sigma_{NO2R} \quad (2)$$

$$X_{Tnorm} = (X_T - \mu_T)/\sigma_T \quad (3)$$

$$X_{RHnorm} = (X_{RH} - \mu_{RH})/\sigma_{RH} \quad (4)$$

$$Y_{O3RSnorm} = (Y_{O3RS} - \mu_{O3RS})/\sigma_{RS} \quad (5)$$

$$Y_{O3RSnorm} = \beta_0 + \beta_{O3}X_{O3Rnorm} + \beta_T X_{Tnorm} + \beta_{RH}X_{RHnorm} \quad (6)$$

$$Y_{O3RSnorm} = \beta_0 + \beta_{NO2}X_{NO2Rnorm} + \beta_{O3}X_{O3Rnorm} + \beta_T X_{Tnorm} + \beta_{RH}X_{Rhnorm} + \varepsilon \quad (7)$$

where parameters μ_{O3RS}, μ_{O3R}, μ_{NO2R}, μ_T and μ_{RH} are the means of the reference station data (μg/m^3), resistor (metal-oxide) or voltage (electro-

Table 2
Correlation coefficient and linear regression coefficients of sensor vs. reference data.

Hourly average				
Captor node	Location	Correlation (R^2)	Slope	Intercept
17001	Manlleu	0.91	0.91	6.97
17002	Manlleu	0.87	0.83	14.21
17003	Manlleu	0.93	0.94	3.76
17005	Manlleu	0.94	0.94	3.59
17010	Manlleu	0.91	0.91	5.24
17011	Manlleu	0.90	0.91	5.57
17013	**Manlleu**	**0.88**	**0.79**	**14.31**
17004	Tona	0.96	0.99	−0.08
17006	Tona	0.84	0.75	18.72
17007	Tona	0.85	0.74	18.48
17012	Tona	0.93	0.96	1.58
17014	Tona	0.88	0.84	11.05
17017	**Tona**	**0.84**	**0.74**	**22.68**
17022	Tona	0.78	0.72	28.85
17023	Tona	0.90	0.81	17.39
17025	Tona	0.95	0.93	0.99
17027	Tona	0.92	0.90	5.96
17009	**Palau Reial**	**0.83**	**0.94**	**8.99**
17015	Palau Reial	0.87	0.85	9.93
17018	Palau Reial	0.86	0.87	8.88
17019	Palau Reial	0.85	0.81	13.70
17020	Palau Reial	0.87	0.90	8.74
17026	Palau Reial	0.87	0.84	10.03
17016	**Vic**	**0.89**	**0.96**	**12.21**
17021	**Montseny**	**0.92**	**0.84**	**12.77**
17024	Cuneo	0.83	0.86	11.82
17029	Cuneo	0.84	0.79	11.41
17031	**Cuneo**	**0.83**	**0.91**	**3.84**
17028	Monte Cucco	0.88	0.89	9.52
17033	**Monte Cucco**	**0.89**	**0.90**	**2.91**
17034	Monte Cucco	0.87	0.92	6.76
17030	Colli Euganei	0.81	0.78	21.23
17035	**Osio Sotto**	**0.90**	**0.93**	**−4.88**
Hourly average				
Raptor node	Location	Correlation (R^2)	Slope	Intercept
69	**Monte Cucco**	**0.88**	**0.90**	**15.32**
216	Monte Cucco	0.90	0.94	−0.55
204	Cuneo	0.73	0.85	10.76
210	Cuneo	0.82	0.78	21.21
202	**Colli Euganei**	**0.83**	**0.90**	**2.13**
206	Colli Euganei	0.92	0.92	3.96
208	Colli Euganei	0.93	0.95	−0.35
212	Osio Sotto	0.93	0.99	−7.92
214	Osio Sotto	0.95	0.94	6.54
218	Osio Sotto	0.90	0.90	−3.30
70	**Palau Reial**	**0.89**	**0.95**	**−4.49**
70	**Tona**	**0.96**	**0.92**	**1.67**

Table 3
Summary statistics of correlation coefficients for all Captor and Raptor nodes.

Correlation (R^2)	All Captors	All Raptors
Number of nodes	33	11
Mean	0.88	0.89
Median	0.88	0.90
Max	0.96	0.96
Min	0.78	0.73

chemical) of ozone or nitrogen dioxide sensors (KOhm or Volts), T (°C) and RH (%) respectively. Parameters σ_{O3RS}, σ_{O3R}, σ_{NO2R}, σ_T and σ_{RH} are the standard deviation for the same parameters. Parameters X_{O3R}, X_{NO2R}, X_T, X_{RH} are the data measured in the low-cost sensors, Y_{O3RS} is the reference station ozone concentration and ε is the error, Gaussian distributed with mean zero and variance σ^2, i.e., $\varepsilon \sim N(0, \sigma^2)$.

As a result of this calibration process, four time-series of ozone concentrations were obtained for each Captor node during each of the calibration periods, and one time-series per calibration period for each Raptor node. All of these time series were then compared with the simultaneous reference ozone concentrations, and the root mean square error (RMSE) was calculated for each individual sensor during each co-located period (143 sensors; Table S2). The RMSE was used to identify the best performing sensor during each calibration period, to assess potential differences in performance between both calibration periods (e.g., drifts), as well as to compare the performance between Captor and Raptor nodes. The final ozone concentration for each of the Captor nodes was selected as that of the best performing sensor. The initial intention was to apply a clustering approach in order to combine the different sensor signals within a single node to calculate the final ozone concentration time series (Smith et al., 2017). However, it was observed that the errors of the different sensors were correlated, and therefore applying a fusion algorithm did not reduce the RMSE. As a result, a single-sensor approach was used instead.

3. Results and discussion

3.1. Comparison between raw sensor and reference ozone data

As described in the previous section, the first phase of the calibration process involved correlating raw sensor data (in electrical resistance units) with simultaneous reference ozone concentrations (μg/m^3). The correlation coefficients (R^2) between raw sensor and reference data and their distribution are shown in Fig. 3. For the Captor sensors, the R^2 ranged between 0.10 and 0.89, with 16 out of 132 sensors showing a correlation <0.10 during the first calibration (Fig. 3). During the second calibration it ranged between 0.10 and 0.95, and only 1 out of 132 sensors had a correlation <0.10 (Fig. 3). This analysis evidences that results improved during the second calibration period (September–October) with regard to the first (May–June), which was interpreted as resulting from the lower ambient ozone concentrations registered after the summer (e.g., mean ozone at Tona reference station = 80 μg/m^3 in May–June with 189 μg/m^3 hourly maximum, vs. 49 μg/m^3 in September–October with 128 μg/m^3 hourly maximum). It is known that metal-oxide sensors generally underestimate high ozone concentrations (Moltchanov et al., 2015; Spinelle et al., 2015a, b; WMO, 2018), and as a result perform better (when compared with reference instruments) when exposed to lower ambient concentrations. R^2 coefficients obtained for Raptor sensors ranged between 0.31 and 0.98, with only 1 out of 11 sensors showing a correlation <0.75 during the first calibration (Fig. 3). During the second calibration they ranged between 0.48 and 0.98 with 3 out of 11 sensors having a correlation <0.75 (Fig. 3). Because electrochemical sensors do not suffer from the same limitations as metal-oxide sensors when challenged with high concentrations, similar results were obtained for Raptor sensors during both calibrations. This is also probably related to the fact that the response of electrochemical sensors with T and RH is more linear than that of metal-oxide sensors (Moltchanov et al., 2015; WMO, 2018).

When plotting the raw sensor against reference ozone data for each of the calibration periods, the performance of individual sensors varied largely from unit to unit. Selected examples for two Captor and two Raptor sensors are shown in Fig. 4, and the results for all of the sensors (132 metal-oxide and 11 electrochemical) are shown in Supporting information (Fig. S2 and Table S2). Whereas for some of the sensors slope of the regression line remained stable for both calibration periods (e.g., Captor #17004-sensor 4, and Raptor 208; Fig. 4), suggesting an apparent absence of drifts, for others a clear change in the slope was detected (e.g., Captor #17007-sensor 3, and Raptor 218; Fig. 4). In the latter cases, the performance of some sensors decreased over time while it improved for others, and thus these changes could not be ascribed to sensor deterioration over time. Prior experiences in this research project (data from 2016, not shown) suggested that sensor signal stability may have been influenced by physical transport of the nodes to and from measurement locations, as components inside the nodes shifted: however, in the period reported in this work this was not the case (components were fixed properly inside the boxes), given that several of the nodes were transported to other monitoring locations between first and second calibration periods and their signals remained stable. In general, the decreasing performance of sensors is frequently observed (WMO, 2018) and may be attributed to internal drifts due to manufacturing process (Moltchanov et al., 2015; Spinelle et al., 2015a, b, 2017) and or to sensors ageing. As stated above, for some sensors in this work the drifts resulted (unexpected) in improvements in performance (e.g. Captor #17012-sensor 4 or #17015-sensor 1; Fig. S2).

Further research is currently underway aiming to understand the different performance of the sensors over time and in producing better

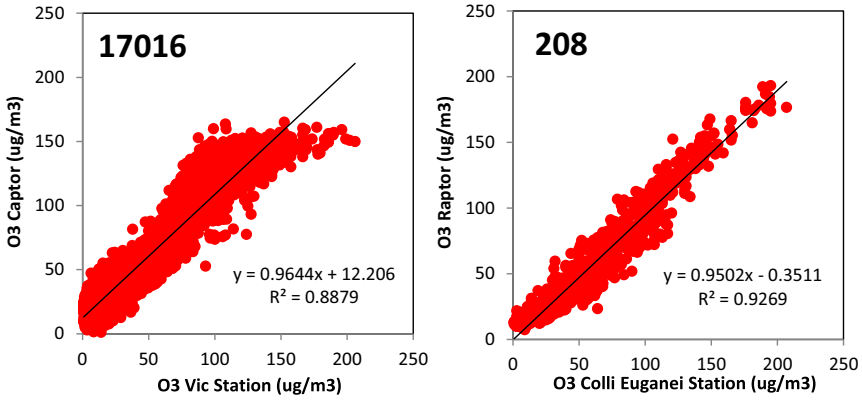

Fig. 6. Scatter plots of hourly ozone concentrations: reference vs. sensor data (metal-oxide, left; electrochemical, right) for the summer period at reference stations in Spain (26/05/2017–05/10/2017) and Italy (29/06/2017–14/07/2017 and 06/10/2017–25/10/2017).

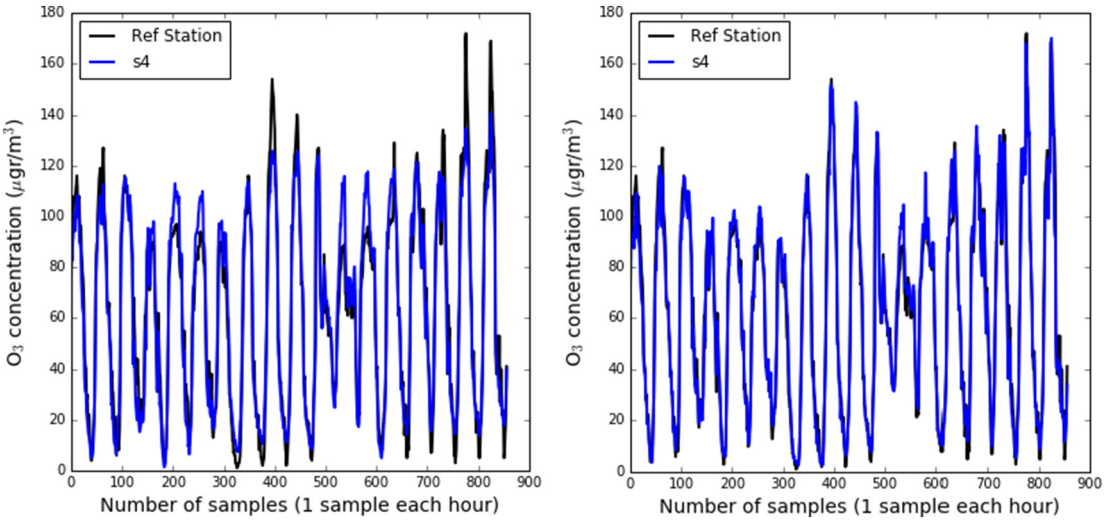

Fig. 7. Comparison between the results from a linear (left) and a non-linear (right) calibration method, tested for a subset of data (850 data points, hourly means, from node 17001, sensor 4).

estimator algorithms. As shown above, Fig. 4 (Captor #17007) indicates that the response during the second calibration can be linked to different environmental conditions in terms of lower average ozone concentrations and different average temperature and relative humidity than during the first calibration period. A research challenge is the possibility of predicting long-term ozone concentrations (e.g., 2–3 months in the future) using a short calibration period (around 3 weeks). This would imply predicting ozone concentrations while correcting for variability

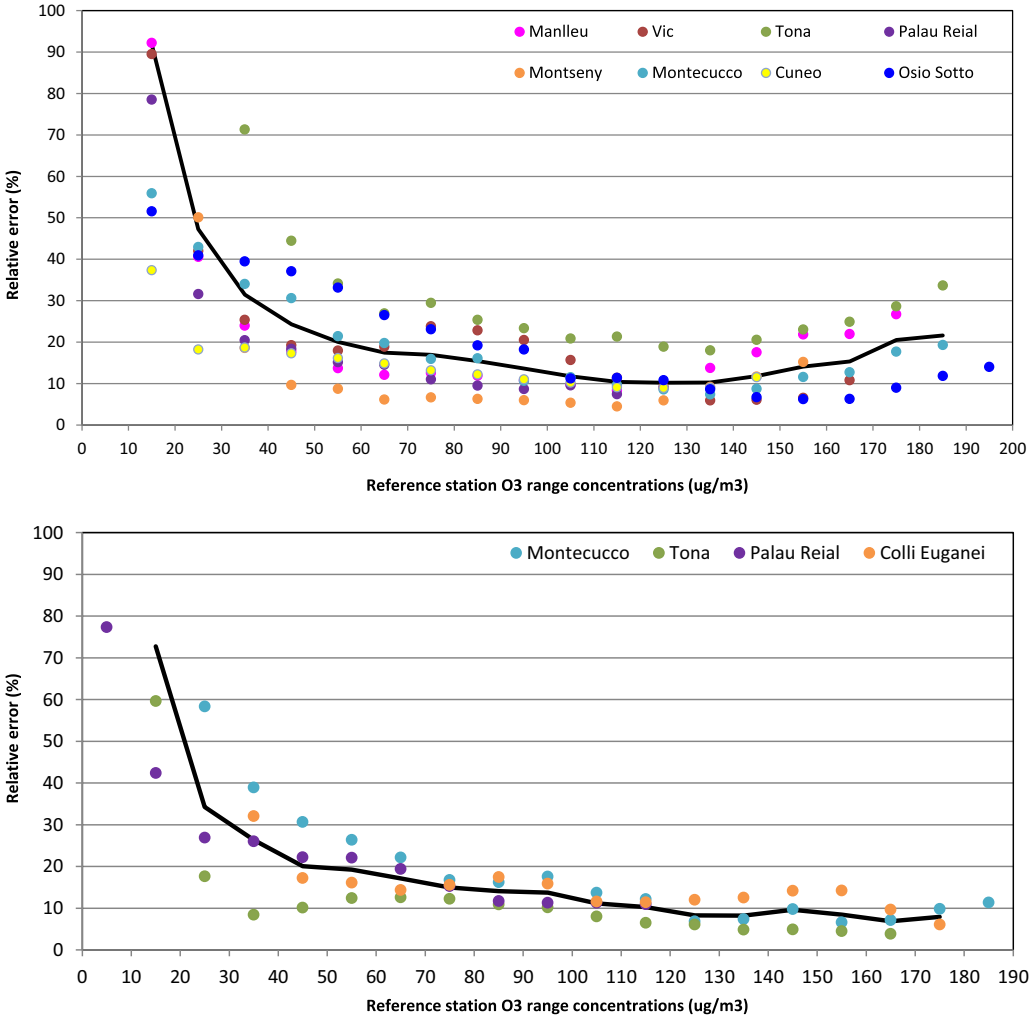

Fig. 8. Relative uncertainty (%) of Captor (top) and Raptor (bottom) nodes as a function of reference ozone concentrations.

linked to environmental conditions, not to drifts linked to technical issues. This work is currently underway, and studies on this are already available (Kizel et al., 2018).

3.2. Root mean square errors (RMSE)

As described in the Methodology, MLR analysis was applied to the sensor raw data using the reference ozone concentrations as independent variable in order to obtain the beta coefficients necessary to convert the sensor raw data to ozone concentrations (in μg/m^3). The ozone time series obtained from the sensors were then compared to the reference data, and the root mean square error (RMSE) was calculated for each individual sensor during both calibration periods (Fig. 5 and Table S2). For each node 4 RMSEs are presented, one for each of the sensing units. The RMSE are presented as absolute (μg/m^3) and not relative (%) concentrations in order to avoid the influence of the higher vs. lower ozone reference concentrations in May–June vs. September–October.

Captor sensors showed RMSEs between 9 and 26 μg/m^3 during the first calibration and between 7 and 19 μg/m^3 during the second calibration period (Fig. 5). The higher RMSEs obtained for the first calibration period seem to confirm the poorer performance of the metal-oxide sensors when challenged with high concentrations, when compared to the lower concentrations recorded in September–October. RMSEs obtained for the lower concentration ranges were similar for both calibration periods (7–9 μg/m^3). In the case of Raptor nodes (electrochemical sensors), the RMSEs obtained ranged between 6 and 17 μg/m^3 (first calibration) and 5–14 μg/m^3 (second calibration) and were thus relatively comparable to those obtained for Captor nodes (metal-oxides) for the second calibration period, i.e., for the lower concentration range (e.g., mean ozone at Tona reference station = 48.7 μg/m^3 in September–October with 128 μg/m^3 hourly maximum). The RMSEs

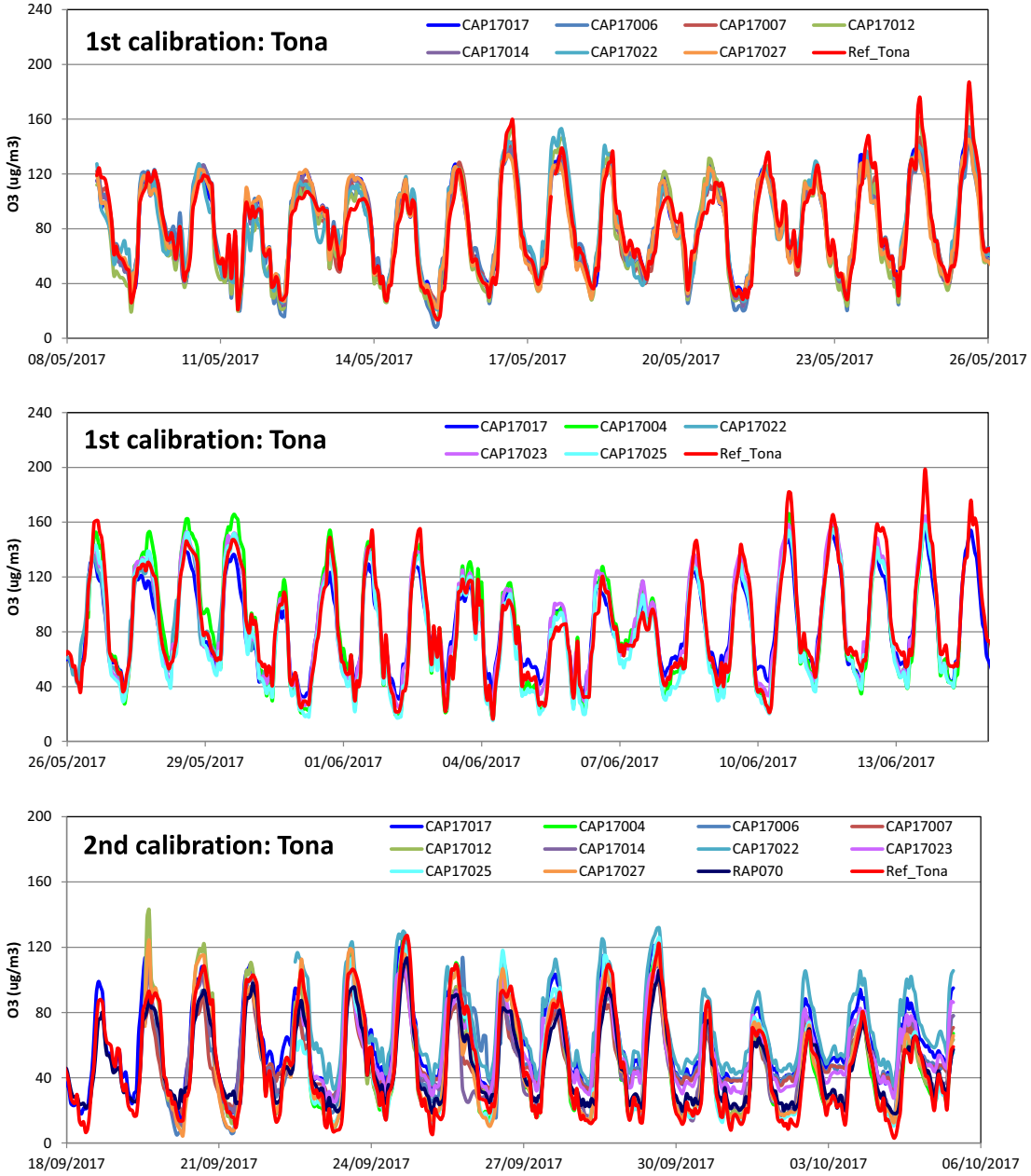

Fig. 9. Ozone time series for co-located ozone Captor nodes, during the first and second calibration periods.

from the Raptor nodes showed a lower variability across calibration periods, thus evidencing a better performance for higher ozone concentrations and a lower influence of ambient conditions.

Intra-nodal variability of the RMSEs was also assessed for Captor nodes (4 sensors). Even though a limited number of nodes showed similar RMSEs for all sensors (e.g. #17022 during the first calibration, or #17009 during both calibrations), the overall trend showed a 5–7 μg/m^3 difference between sensors in a given node. This would be the uncertainty associated to using a single-sensor approach for the quantification of ozone concentrations as opposed to a clustering approach (Kizel et al., 2018; Smith et al., 2017).

3.3. Selection of final ozone time series and performance testing

The RMSEs quantified for each individual sensor were used to select the best performing sensor, which was the one with the lowest RMSE. In addition, for the best performing sensor, the beta coefficients (obtained from MLR analysis) obtained for each of the calibration periods were assessed in order to select the coefficients which better reproduced ozone concentrations under high (May–June) and low (September–October) ambient ozone concentrations. Based on these assessments (RMSE and MLR coefficients from each of the calibration periods), the final ozone time series for each of the Captor nodes were selected.

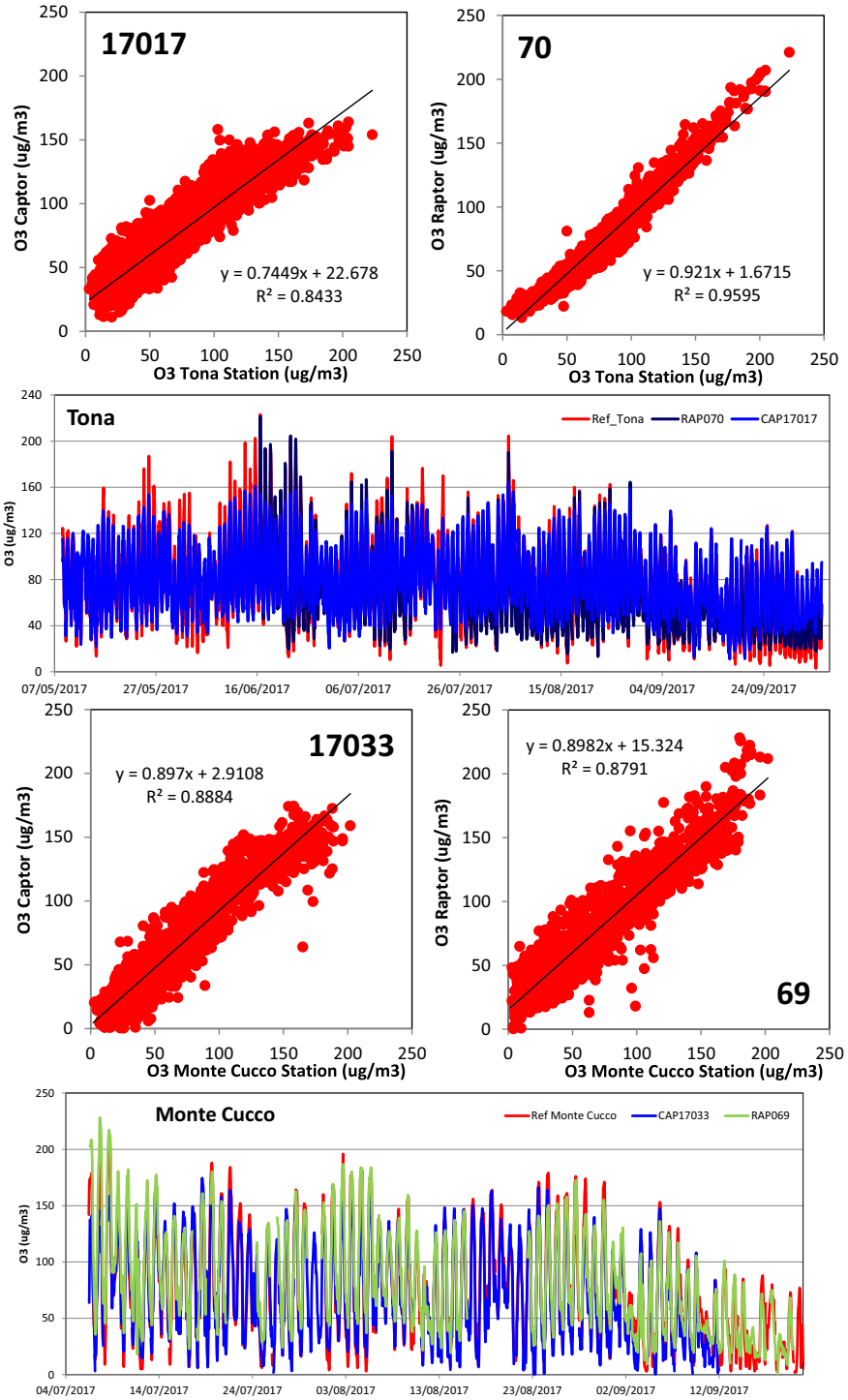

Fig. 10. Long-term co-located deployment of Captor and Raptor nodes in Spain (top) and Italy (bottom), and comparison with reference ozone concentrations.

This process was not necessary for the Raptor nodes as they only contained one sensing unit each.

The comparison between the reference and sensor ozone time series, for selected Captor and Raptor nodes, is shown in Fig. 5. The results for the 33 Captor and 11 Raptor nodes analysed in this work (143 individual sensors in total) are shown in Table 2 and in Supporting information (Figs. S3 and S5). As shown in the tables, when applying a calibration strategy such as the one described in this work, mean R^2 values for all nodes were comparable for the 33 Captors and 11 Raptors tested ($R^2 = 0.88$ and 0.89, respectively, Table 3). The minimum and maximum R^2 values were also similar for both types of sensors (0.73–0.78, and 0.96, respectively), with a slightly higher median for Raptor nodes (0.90, vs. 0.88 for Captor nodes). These results were irrespective of the sample size, given that similar results were obtained for the nodes which were collocated for 5 months (highlighted in bold in Table 2) and those collocated for 1 month (only during the calibration periods).

This assessment, which is based strictly on mean R^2 values, does not allow to conclude a better performance of the electrochemical sensors (compared to the metal-oxide ones) when exposed to higher concentrations. However, Fig. 6 shows that the metal-oxide sensors in the Captor nodes seemed to have an upper limit around 170 μg/m^3, which is not the case for the electrochemical sensors in the Raptors (at least within the concentration range to which the nodes were exposed; Fig. 6), which were able to measure higher ozone concentrations (>200 μg/m^3). With regard to the lower detection limit, both types of nodes (Captor and Raptor) seemed to report reliable concentrations down to approximately 20–30 μg/m^3, with smaller differences between both types of sensors. The results for all of the nodes are shown in the Supporting information (Figs. S4 and S5). These findings are consistent with the literature (Moltchanov et al., 2015; Spinelle et al., 2015a, b; Kizel et al., 2018; WMO, 2018), where the non-linear response of the metal-oxide sensors is already described. While the literature reports this limitation based on studies which apply linear models for sensor calibration (WMO, 2018; and references therein), the large dataset available in the present work (>4 month time series; 132 metal-oxide sensors) could be sufficient to evidence that this limitation could be overcome by applying non-linear regression models to calibrate metal-oxide sensors. Work is currently underway in this research direction.

A preliminary evaluation of the potential of non-linear regression was carried out by comparing the results from the linear calibration (MLR; Fig. 7 left) and non-linear calibration (SVR, Support Vector Regression; Fig. 7 right) of a subset of data (850 data points, hourly means, from node 17001, sensor 4). The model SVR (Esposito et al., 2017) uses a similar approach to artificial neural networks (ANN; Spinelle et al., 2017). Preliminary results for this subset of data were that the calibration with MLR (linear) resulted in an RMSE of 9.1 μg/m^3 with $R^2 = 0.95$, while the non-linear calibration (SVR) had lower RMSE (6.2 μg/m^3) and higher R^2 (0.98). The main advantage of the SVR calibration was its ability to reproduce high hourly concentrations (Fig. 7): while the linear calibration of the CAPTOR node was unable to reach the highest means (left), with the non-linear calibration these were adequately reproduced by the model. Calibration of the lowest hourly means also improved with the non-linear method, although to a lower extent than the highest means (Fig. 7).

Consequently, based on these results it may be concluded that the performance of the metal-oxide sensors tested in this work could be considered adequate for raising awareness about daily ozone means, but that the sensors would not be adequate to monitor high ozone concentrations during ozone episodes.

Because of the different performance of sensors at different pollutant concentrations, the absolute and relative uncertainty of the Captor and Raptor data with regard to the reference concentrations was quantified for different ozone concentration ranges (Figs. 8 and S6). According to this analysis, the absolute uncertainty of Captor nodes (i.e., including the uncertainty of the sensing units and of the calibration method) was around 10–12 μg/m^3 for ambient ozone concentrations between 30 and 100 μg/m^3, while it increased to 15 μg/m^3 for concentrations 100–150 μg/m^3 and was maximal (from 20 to 40 μg/m^3) for concentrations in the range 150–200 μg/m^3. The uncertainty of Raptor nodes was 8–12 μg/m^3 for concentrations 30–100 μg/m^3 and around 10–15 μg/m^3 for concentrations >100 μg/m^3.

3.4. Intra-node variability

Final time series of ozone concentrations from Captor and Raptor nodes during collocated periods at reference stations are depicted in Fig. 9 (selected examples) and Fig. S4 in Supporting information. In Fig. 9, the different nodes followed comparable daily patterns, similar to that of the simultaneous reference station: diurnal cycles with increasing concentrations during the morning, peaking at midday and decreasing in the afternoon. During the first calibration period the intra-node variability was low (maximum hourly difference between nodes = 5 μg/m^3), with high precision. However, precision decreased significantly during the second calibration period (maximum hourly difference between nodes = 20 μg/m^3), while the accuracy increased due to the lower ozone ambient concentrations. This resulted in better sensor performance for the daily maxima. As discussed above, this decrease in precision could be related to ageing of the sensors, although further research would be necessary to fully understand the nature of these drifts.

3.5. Long-term performance analysis

With the aim to evaluate the long-term performance of both types of sensors, 8 Captor and 4 Raptor nodes (32 metal-oxide and 4 electrochemical ozone sensors) were deployed at reference stations during the entire duration of the study (between 5 and 2.5 months depending on each case). The results are shown in Fig. 10 for 2 examples (1 station in Spain and 1 in Italy), and for all of the stations in Fig. S5. Different stations and countries were selected in Fig. 10 in order to challenge the sensors with different ozone concentrations and ambient meteorological conditions.

The time series analysis of Captor and Raptor data, as well as the scatter plots, evidence a good comparability between sensor and reference data across the 5 study months and under the different environmental conditions in the Italian and Spanish reference stations. R^2 coefficients were 8.84–0.89 for the Captor nodes and 0.88–0.96 for the Raptor nodes, which are within the range obtained for the calibration periods (0.78–0.96 for Captors and 0.73–0.96 for Raptors, Table 3). Thus, during the continued 5-month period the performance of the Captor and Raptor nodes seemed stable and comparable to that during the calibration periods (1–2 months), with no indication of drifts due to ageing of the sensors. This does not mean, however, that drifts may appear after longer periods of time (>5 months). The time series in Fig. 10 show that the comparability between sensor and reference data was maintained during high and low ozone periods, corresponding to the middle and end of the summer.

4. Summary and conclusions

The performance of two types of custom-made sensor nodes for ozone monitoring in a citizen science approach was assessed in this work. The sensors aimed to fulfil the purpose of awareness raising, and were thus not meant for compliance checking or air quality reporting. The sensing nodes were equipped with metal-oxide (referred to as Captor nodes, 33 units tested, 132 individual ozone sensors) and electrochemical (referred to as Raptor nodes, 11 units tested, 11 individual ozone and 11 individual NO_2 sensors) sensors. They were tested in the field by collocation at reference air quality monitoring stations,

and were exposed to different ambient ozone concentrations and environmental conditions in Italy and Spain.

The individual sensor datasets were calibrated applying multi-linear regression (MLR) analysis, which resulted in mean R^2 between calibrated sensor and reference data of 0.88 and 0.89 for Captor and Raptor nodes, respectively (with ranges 0.78–0.96 for Captors and 0.73–0.96 for Raptors). These results support the validity of the calibration approach applied. However, the metal-oxide sensors seemed to have an upper concentration limit (approximately 170 μg/m^3) which was not the case for the electrochemical sensors. This behaviour was consistent with the literature. For this reason, metal-oxide sensors may be useful in citizen science approaches to communicate mean ozone concentrations, but not peak episodes. In order to overcome this limitation, non-linear regression models are probably better suited than linear ones to calibrate metal-oxide sensors. Linear ones are adequate for calibration of electrochemical sensors.

The relative uncertainty of the Captor nodes with regard to the reference concentrations was quantified, as a function of ambient ozone concentrations to account for the upper limit described above. This uncertainty was around 10% for ambient ozone concentrations between 100 and 150 μg/m^3, while it increased to 20% for concentrations 150–200 μg/m^3. The relative uncertainty of Raptors nodes was 10% for concentrations >100 μg/m^3. The long-term performance (up to 5 months) of both types of nodes was comparable to that in the short-term (1–2 months), with no evidence of drifts over time.

Based on these results, it may be concluded that the performance of the metal-oxide sensors tested in this work is considered adequate for reporting daily ozone means for awareness raising, but that the sensors would not be adequate for communicating high summer midday ozone episodes typical of the Mediterranean region, with the calibration methods used in this work. Thus, over all, the use of these sensors in a citizen science can be a useful tool for awareness raising. The data processing effort required implies that, for the sensing nodes tested in this work, the application of machine learning strategies would be advisable. The relative uncertainties quantified in this work should always be taken into account when reporting ozone concentration data from Captor and Raptor sensing nodes.

Acknowledgements

The authors would like to thank the anonymous reviewers, whose comments improved the manuscript significantly. This work was funded by H2020 project CAPTOR. The authors gratefully acknowledge the collaboration of the staff at the Department of the Environment of the Generalitat de Catalunya and at ARPA Lombardia (Agenzia Regionale per l'Ambiente), who kindly provided support for the deployment of the sensing nodes at reference stations and provided access to the reference data. Support is also acknowledged from AGAUR SGR44, the Agencia Estatal de Investigación (AEI; CGL2017-82093-ERC), and the Spanish Ministry of Economy, Industry and Competitiveness (EUIN2017-85799).

Appendix A. Supplementary data

Supplementary data to this article can be found online at https://doi.org/10.1016/j.scitotenv.2018.09.257.

References

Aleixandre, M., Gerboles, M., 2012. Review of small commercial sensors for indicative monitoring of ambient gas. Chem. Eng. Trans. 30, 169–174.
Borghi, F., Spinazzè, A., Rovelli, S., Campagnolo, D., Del Buono, L., Cattaneo, A., Cavallo, D.M., 2017. Miniaturized monitors for assessment of exposure to air pollutants: a review. Int. J. Environ. Res. Public Health https://doi.org/10.3390/ijerph14080909.
Broday, D.M., Citi-Sense, Collaborators, P, 2017. Wireless distributed environmental sensor networks for air pollution measurement—the promise and the current reality. Sensors 17.
Cristofanelli, P., Bonasoni, P., 2009. Background ozone in the southern Europe and Mediterranean area: influence of the transport processes. Environ. Pollut. 157, 1399–1406. https://doi.org/10.1016/j.envpol.2008.09.017.
EEA, 2017. Air Quality in Europe, EEA Report No 13/2017. https://doi.org/10.2800/358908.
Esposito, E., De Vito, S., Salvato, M., Fattoruso, G., Di Francia, G., 2017. Computational intelligence for smart air quality monitors calibration. International Conference on Computational Science and Its Applications. Springer, Cham, pp. 443–454.
ETC, 2018. Ozone in Southern Europe - Assessment and Effectiveness of Measures. Authors: Mar Viana, Marc Padrosa, Xavier Querol, Andrés Alastuey, Nina Benesova, Blanka Krejčí, Vladimíra Volná, Elsa Real, Augustin Colette, Frank de Leeuw, Alberto González Ortiz (doi: ETC/ACM Technical Paper 2017/3).
European Environment Agency, 2017. Air Quality in Europe, EEA Report No 13/2017. https://doi.org/10.2800/358908.
Gangoiti, G., Millán, M.M., Salvador, R., Mantilla, E., 2001. Long-range transport and recirculation of pollutants in the Western Mediterranean during the project Regional Cycles of Air Pollution in the West-Central Mediterranean Area. Atmos. Environ. 35, 6267–6276.
Gerasopoulos, E., Kouvarakis, G., Vrekoussis, M., Donoussis, C., Mihalopoulos, N., Kanakidou, M., 2006. Photochemical ozone production in the Eastern Mediterranean. Atmos. Environ. 40, 3057–3069. https://doi.org/10.1016/j.atmosenv.2005.12.061.
Haklay, M., 2015. Citizen Science and Policy: A European Perspective.
Hastie, T., Friedman, J., Tibshirani, R., 2001. The Elements of Statistical Learning. Springer Series in StatisticsSpringer New York, New York, NY https://doi.org/10.1007/978-0-387-21606-5.
HEI, 2017. Multicenter Ozone Study in oldEr Subjects (MOSES): Part 1. Effects of Exposure to Low Concentrations of Ozone on Respiratory and Cardiovascular Outcomes.
Hubbell, B., Kaufman, A., Rivers, L., Schulte, K., Hagler, G., Clougherty, J., Cascio, W., Costa, D., 2018. Understanding social and behavioral drivers and impacts of air quality sensor use. Sci. Total Environ. 621, 886–894.
Jiao, W., Hagler, G., Williams, R., Sharpe, R., Brown, R., Garver, D., Judge, R., Caudill, M., Rickard, J., Davis, M., Weinstock, L., Zimmer-Dauphinee, S., Buckley, K., 2016. Community Air Sensor Network (CAIRSENSE) project: evaluation of low-cost sensor performance in a suburban environment in the southeastern United States. Atmos. Meas. Tech. 9, 5281–5292.
Kizel, F., Etzion, Y., Shafran-Nathan, R., Levy, I., Fishbain, B., Bartonova, A., Broday, D.M., 2018. Node-to-node field calibration of wireless distributed air pollution sensor network. Environ. Pollut. 233, 900–909. https://doi.org/10.1016/j.envpol.2017.09.042.
Lewis, A., Edwards, P., 2016. Validate personal air-pollution sensors. Nature 535, 29–31.
Lewis, A.C., Lee, J., Edwards, P., Shaw, M., Evans, M., Moller, S., Smith, K., Buckley, J., M., E., SR, G., White, A., 2016. Evaluating the performance of low cost chemical sensors for air pollution research. Faraday Discuss.
Lin, C., Gillespie, J., Schuder, M.D., Duberstein, W., Beverland, I.J., Heal, M.R., 2015. Evaluation and calibration of Aeroqual series 500 portable gas sensors for accurate measurement of ambient ozone and nitrogen dioxide. Atmos. Environ. 100, 111–116. https://doi.org/10.1016/j.atmosenv.2014.11.002.
Lin, C., Masey, N., Wu, H., Jackson, M., Carruthers, D.J., Reis, S., Doherty, R.M., Beverland, I.J., Heal, M.R., 2017. Practical field calibration of portable monitors for mobile measurements of multiple air pollutants. Atmosphere (Basel) 8, 1–19. https://doi.org/10.3390/atmos8120231.
Mészáros, E., 1999. Fundamentals of Atmospheric Aerosol Chemistry. Akadémiai Kiado, Budapest.
Millán, M.M., Artíñano, B., Alonso, L., Navazo, M., Castro, M., 1991. The effect of meso-scale flows and long range atmospheric transport in the western Mediterranean area. Atmos. Environ. 25, 949–963.
Millán, M., Mantilla, E., Salvador, R., Carratalá, A., Sanz, M.J., Alonso, L., Gangoiti, G., Navazo, M., 2000. Ozone cycles in the Western Mediterranean basin: interpretation of monitoring data in complex coastal terrain. J. Appl. Meteorol. 39, 487–508.
Moltchanov, S., Levy, I., Etzion, Y., Lerner, U., Broday, D.M., Fishbain, B., 2015. On the feasibility of measuring urban air pollution by wireless distributed sensor networks. Sci. Total Environ. 502, 537–547. https://doi.org/10.1016/j.scitotenv.2014.09.059.
Monks, P.S., Archibald, A.T., Colette, A., Cooper, O., Coyle, M., Derwent, R., Fowler, D., Granier, C., Law, K.S., Mills, G.E., Stevenson, D.S., Tarasova, O., Thouret, V., von Schneidemesser, E., Sommariva, R., Wild, O., Williams, M.L., 2015. Tropospheric ozone and its precursors from the urban to the global scale from air quality to short-lived climate forcer. Atmos. Chem. Phys. 15, 8889–8973. https://doi.org/10.5194/acp-15-8889-2015.
Morawska, L., Thai, P.K., Liu, X., Asumadu-Sakyi, A., Ayoko, G., Bartonova, A., Bedini, A., Chai, F., Christensen, B., Dunbabin, M., Gao, J., Hagler, G.S.W., Jayaratne, R., Kumar, P., Lau, A.K.H., Louie, P.K.K., Mazaheri, M., Ning, Z., Motta, N., Mullins, B., Rahman, M.M., Ristovski, Z., Shafiei, M., Tjondronegoro, D., Westerdahl, D., Williams, R., 2018. Applications of low-cost sensing technologies for air quality monitoring and exposure assessment: how far have they gone? Environ. Int. 116, 286–299. https://doi.org/10.1016/j.envint.2018.04.018.
Mukherjee, A., Stanton, L.G., Graham, A.R., Roberts, P.T., 2017. Assessing the utility of low-cost particulate matter sensors over a 12-week period in the Cuyama Valley of California. Sensors 17.
Nakayama, T., Matsumi, Y., Kawahito, K., Watabe, Y., 2017. Development and evaluation of a palm-sized optical $PM_{2.5}$ sensor. Aerosol Sci. Technol. 6826, 1–11. https://doi.org/10.1080/02786826.2017.1375078.
Nali, C., Pucciariello, C., Lorenzini, G., 2002. Mapping O_3 critical levels for vegetation in Central Italy. Water Air Soil Pollut. 141, 337–347.
Pusede, S.E., Steiner, A.L., Cohen, R.C., 2015. Temperature and recent trends in the chemistry of continental surface ozone. Chem. Rev. 115, 3898–3918. https://doi.org/10.1021/cr5006815.

Querol, X., Alastuey, A., Reche, C., Orio, A., Pallares, M., Reina, F., Dieguez, J.J., Mantilla, E., Escudero, M., Alonso, L., Gangoiti, G., Millán, M., 2016. On the origin of the highest ozone episodes in Spain. Sci. Total Environ. 572, 379–389. https://doi.org/10.1016/j.scitotenv.2016.07.193.

Querol, X., Gangoiti, G., Mantilla, E., Alastuey, A., Minguillón, M.C., Amato, F., Reche, C., Viana, M., Moreno, T., Karanasiou, A., Rivas, I., Pérez, N., Ripoll, A., Brines, M., Ealo, M., Pandolfi, M., Lee, H.K., Eun, H.R., Park, Y.H., Escudero, M., Beddows, D., Harrison, R.M., Bertrand, A., Marchand, N., Lyasota, A., Codina, B., Olid, M., Udina, M., Jiménez-Esteve, B., Jiménez-Esteve, B.B., Alonso, L., Millán, M., Ahn, K.H., 2017. Phenomenology of high-ozone episodes in NE Spain. Atmos. Chem. Phys. 17, 2817–2838. https://doi.org/10.5194/acp-17-2817-2017.

Rai, A.C., Kumar, P., Pilla, F., Skouloudis, A.N., Di Sabatino, S., Ratti, C., Yasar, A., Rickerby, D., 2017. End-user perspective of low-cost sensors for outdoor air pollution monitoring. Sci. Total Environ. 607–608, 691–705. https://doi.org/10.1016/J.SCITOTENV.2017.06.266.

Richards, N.A.D., Arnold, S.R., Chipperfield, M.P., Miles, G., Rap, A., Siddans, R., Monks, S.A., Hollaway, M.J., 2013. The Mediterranean summertime ozone maximum: global emission sensitivities and radiative impacts. Atmos. Chem. Phys. 13, 2331–2345. https://doi.org/10.5194/acp-13-2331-2013.

Sillman, S., 1999. The relation between ozone, NO_x and hydrocarbons in urban and polluted rural environments. Atmos. Environ. 33, 1821–1845. https://doi.org/10.1016/S1352-2310(98)00345-8.

Smith, K.R., Edwards, P.M., Evans, M.J., Lee, J.D., Shaw, M.D., Squires, F., Lewis, A.C., 2017. Clustering approaches to improve the performance of low cost air pollution sensors. Faraday Discuss. 200, 621–637. https://doi.org/10.1039/C7FD00020K.

Spinelle, L., Gerboles, M., Aleixandre, M., 2015a. Performance evaluation of amperometric sensors for the monitoring of O_3 and NO_2 in ambient air at ppb level. Procedia Eng. 120, 480–483.

Spinelle, L., Gerboles, M., Villani, M., Aleixandre, M., Bonavitacola, F., 2015b. Field calibration of a cluster of low-cost available sensors for air quality monitoring. Part A: ozone and nitrogen dioxide. Sensors Actuators B Chem. 215, 249–257. https://doi.org/10.1016/j.snb.2015.03.031.

Spinelle, L., Gerboles, M., Villani, M.G., Aleixandre, M., Bonavitacola, F., 2017. Field calibration of a cluster of low-cost commercially available sensors for air quality monitoring. Part B: NO, CO and CO_2. Sensors Actuators B Chem. 238, 706–715. https://doi.org/10.1016/j.snb.2016.07.036.

Varinou, M., Kallos, G., Tsiligiridis, G., Sistla, G., 1999. The role of anthropogenic and biogenic emissions on tropospheric ozone formation over Greece. Phys. Chem. Earth Part C 24, 507–513. https://doi.org/10.1016/S1464-1917(99)00081-1.

WHO, 2008. Health Risks of Ozone From Long-range Transboundary Air Pollution. WHO Regional Office for Europe, Scherfigsvej 8 DK-2100 Copenhagen Ø, Denmark.

Williams, D.E., Henshaw, G.S., Bart, M., Laing, G., Wagner, J., Naisbitt, S., Salmond, J.A., 2013. Validation of low-cost ozone measurement instruments suitable for use in an air-quality monitoring network. Meas. Sci. Technol. 24, 65803.

Williams, R., Long, R., Beaver, M., Kaufman, A., Zeiger, F., Heimbinder, M., Hang, I., R., Y., Acharya, B., Ginwald, B., Kupcho, K., Robinson, S., Zaouak, O., Aubert, B., M., H., Piedrahita, R., Masson, N., Moran, B., Rook, M., Heppner, P., Cogar, C., N., N., Griswold, W., 2014. Sensor Evaluation Report.

WMO, 2018. Low-cost Sensors for the Measurement of Atmospheric Composition: Overview of Topic and Future Applications.

Zikova, N., Masiol, M., Chalupa, D.C., Rich, D.Q., Ferro, A.R., Hopke, P.K., 2017. Estimating hourly concentrations of $PM_{2.5}$ across a metropolitan area using low-cost particle monitors. Sensors 17.

Zimmerman, N., Presto, A.A., Kumar, S.P.N., Gu, J., Hauryliuk, A., Robinson, E.S., Robinson, A.L., Subramanian, R., 2018. A machine learning calibration model using random forests to improve sensor performance for lower-cost air quality monitoring. Atmos. Meas. Tech. 11, 291–313. https://doi.org/10.5194/amt-11-291-2018.